CZECH TECHNICAL UNIVERSITY IN PRAGUE

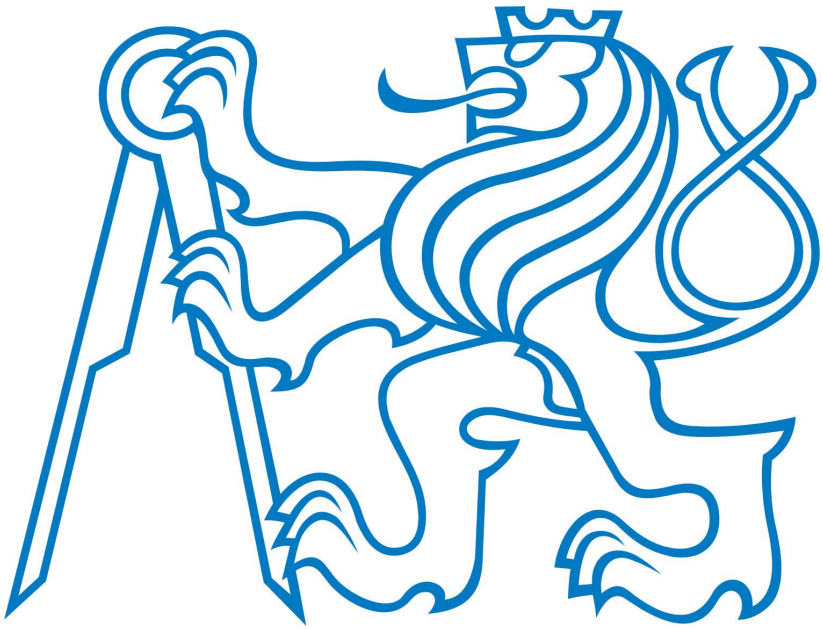

DOCTORAL THESIS STATEMENT

Czech Technical University in Prague

Faculty of Electrical Engineering

Department of Electromagnetic Field

Petr Dvořák

NEW METHODOLOGIES OF REMOTE SENSING BASED ON MICROWAVE RADIOMETER

Ph.D. Programme:
Electrical Engineering and Information Technology

Branch of study: Radioelectronics

Doctoral thesis statement for obtaining the academic title of "Doctor", abbreviated to "Ph.D."

Prague, August 2013

The doctoral thesis was produced in full-time manner Ph.D. study at the department of electromagnetic field of the Faculty of Electrical Engineering of the CTU in Prague

Candidate: Ing. Petr Dvořák

Department of Electromagnetic Field
Faculty of Electrical Engineering of the CTU in Prague
Technická 2, 166 27 Prague 6

Supervisor: Prof. Ing. Miloš Mazánek Csc.

Department of Electromagnetic Field
Faculty of Electrical Engineering of the CTU in Prague
Technická 2, 166 27 Prague 6

Supervisor-Specialist: Doc. Ing. Stanislav Zvánovec Ph.D.

Department of Electromagnetic Field
Faculty of Electrical Engineering of the CTU in Prague
Technická 2, 166 27 Prague 6

Opponents:

The doctoral thesis statement was distributed on:

The defence of the doctoral thesis will be held on ..... at ..... a.m./p.m. before the Board for the Defence of the Doctoral Thesis in the branch of study Radioelectronics in the meeting room No. ..... of the Faculty of Electrical Engineering of the CTU in Prague.

Those interested may get acquainted with the doctoral thesis concerned at the Dean Office of the Faculty of Electrical Engineering of the CTU in Prague, at the Department for Science and Research, Technická 2, Praha 6.

Chairman of the Board for the Defence of the Doctoral Thesis
in the branch of study Radioelectronics
Faculty of Electrical Engineering of the CTU in Prague
Technická 2, 166 27 Prague 6

CURRENT SITUATION OF THE STUDIED PROBLEM

Remote sensing methods have developed over tens of years with rapidly increasing technical maturity. From the beginning the surrounding world was perceived by simple methods by direct human interaction with nature. From the short-range fields (temperature, acoustic) that were observed, investigated and potential trickiness were explained the observations were focused on more and more remote objects from earth atmosphere over the closest space object Moon to planets and stars. Since the direct sensing of these object is very difficult or impossible, only by measuring of long-range fields these remote objects can be effectively examined.

One of the first attempts of remote sensing did Gaspard-Félix Tournachon. Tournachon made first pictures of Earth (Paris) from a balloon. From the year 1858, when the pictures of Paris were created, mankind achieved such technical precocity as is the Plank probe launched in 2009 by the European Space Agency [1]. The probe is equipped with state of the art radiometers scanning the temperature of the universe in three frequency bands from 30 GHz to 70 GHz [24].

For the remote sensing the most convenient means, the electromagnetic field, is mainly used. Sensing of wide frequency spectrum allows to observe the object from various points of view – in terms of sensing of their various states and process by one quantity.

Currently a new types of radiometers are developed and allow us to integrate it to more complex measurement systems. Together with the miniaturization of radiometric systems thanks to MEMS devices and system-on-chip technologies the radiometry becomes a new perspective of remote sensing for satellite, airborne or ground-based scanning.

In this thesis new methodologies of remote sensing will be described. Since the instrumentation for remote sensing is accessible and well developed there are opportunities to propose new methodologies of measuring and dataminig that are crucial in current state of research.

The main aim of this doctoral thesis is to propose new methodologies of remote sensing. The thesis is focused on currently used radiometric methodologies in remote sensing of the terrestrial atmosphere and fire detection and localization. The thesis is organized as follows. After the introduction the second chapter dealing with theoretical background of remote sensing is introduced. At first, principles and fundamentals laws are explained. Currently used radiometers' concepts are also presented. In the third chapter the state of the art in remote sensing is discussed. At first general methodologies of ground-based atmosphere sensing are mentioned. Measuring of atmospheric profiles follows. In relation with atmospheric profiles the precipitation detection and prediction is discussed. The second part of the third chapter is focused on methods of fire detection. In the fourth chapter the thesis objectives are proposed and defined. The main thesis focus consists of two parts, the first part deals with the new methodology of atmosphere dynamic effects (rain, clouds) sensing and is described in chapter . Next, the chapter describes methodology of fire remote detection and it's properties from the microwave point of view.

Rainfall is the key part of hydrological cycle and is under research very long time. Precipitation (especially rainfalls) are accompanied with the heat release which drives significant part of hydrological cycle – the circulation of the atmosphere and water. In this thesis mainly the precipitation above a solid land will be examined.

Ground Based Sensing of Atmosphere

The (passive) atmosphere sensing is mainly performed in visible part of spectrum, infrared and in radio-frequency band. Visible and infrared wave radiated from clouds upwards is often reflected and emitted by top cloud layers and it is insufficiently correlated to the micro-physical structure of clouds bellow the top layer. This is the reason why the visible/infrared information cannot be used satisfactory for rain detection and prediction. Clouds are related with rainfalls mainly in convective systems.

Precipitation Sensing

Having the atmosphere model and profiles the precipitation sensing and prediction can be investigated. In 1999 J. Gueldner performed sensing of water vapor by ground-based radiometer over period of 1 year. Gueldner proposed findings from measuring of precipitable water vapor (PWV) and cloud liquid water (CLW) [10]. The data were measured in central Europe.

A pure state of the art precipitation detection and prediction by a microwave ground-based radiometer was performed by H. Y. Won [28]. For the estimation of rainfall occurrence and intensity a ground based microwave radiometer was used. Ordinary upper-air observation provided by a radioprobe 2 times a day cannot satisfactory substitute local on-line monitoring recording short-time precipitations. By statistical evaluation of measured brightness temperature Gueldner measured increase of PWV and CLW in the time interval of 30 minutes before the rain started. Gueldner has measured the brightness temperature at two channels, 23.8 GHz and 31.4 GHz respectively.

In the Gueldner's work Won continues with his precipitation prediction by a ground-based radiometer [28]. Won has used microwave radiometer that measures 8 water vapor channels in the K-band and 14 oxygen channels in the V-band.

Predictability of precipitation events can be proved by using 15-minute moving data accumulation. If in the 15-minute interval a statistically significant rainfall is detected, it is considered as the rain event. Two datasets are used of the analysis – rain record data set (RR) and no-rain record (NR) dataset. When an event occur and another one occur within 2 hour period after the first one, it is regarded as the same event.

Typical results of Won's method are depicted in Fig. 1. In figures averaged differences of brightness temperature in period of 2 h before the rain starts can be seen. The difference of RR and NR graphs is obvious.

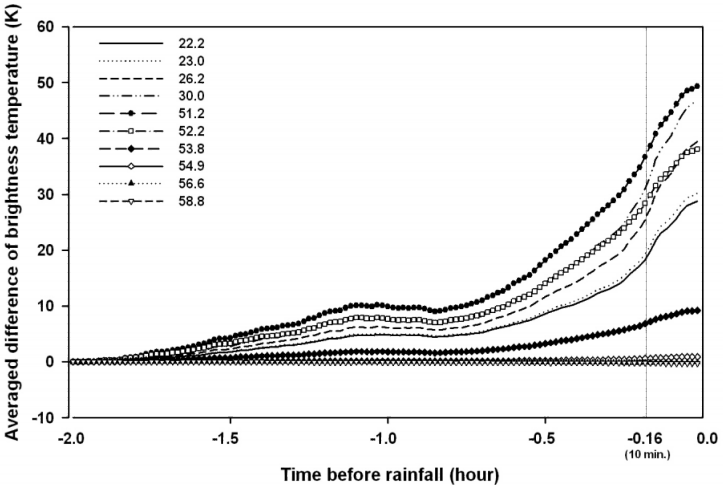

Figure 1: Time averaged brightness temperature differences in 2-hour period before the rain event. RR datasets measured at water vapor frequency channels are used [28].

Methods of Remote Sensing in Case of Fires

As well as the atmosphere can be explored in order to detect and predict undesirable atmospheric effects, fires can be sensed by measuring of thermal radiation too. Every year thousands of square kilometers are burned out because of forest fires causing huge damages on environment and human health. A various fires can be distinguished: fires in buildings, open space fires, fires of dangerous chemical etc. In order to detect fire many way exists where radiometry is one of the interesting tool for this purpose. Currently used fire detectors, from remote sensing point of view, are based on satellite infrared sensors. The problem of infrared sensors is in possible miss of the fire hidden under

a vegetation or other coverage. Since microwaves can penetrate the vegetation layer, which is opaque for visible or IR radiation, radiometers can be successfully used.

Fires Detection

Radiometers for the purpose of fire detection are well designed by the group of F. Alimenti. Alimenti has designed several radiometers for various purposes [11], [2], [3], [23] and the ability to detect a fire was proved. The ability of fire detection was performed by measuring of the open wood fire. For this purpose the microwave radiometer was developed. The working frequency was 12.65 GHz with the bandwidth of 100 MHz. A low-cost radiometer was used to measure thermal radiation in accordance with the European standard EN54. The standard is used to certify optical and temperature fire detectors. In the Fig. 2 the course of experiment is depicted.

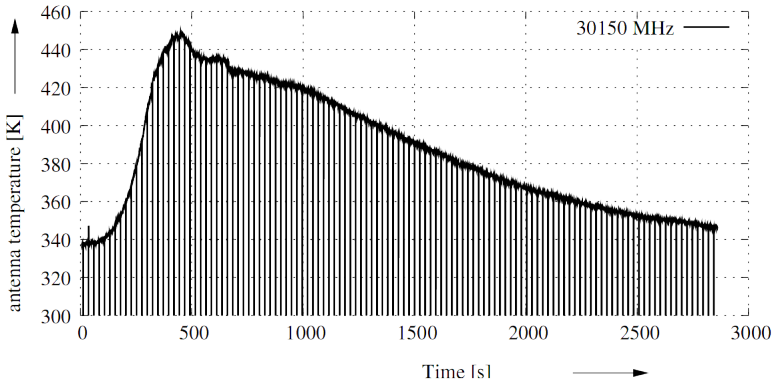

Figure 2: Measured brightness temperature of a wood fire. Experimental procedure performed to prove ability of fire detection in accordance with EN54 standard. The signal dropouts are caused by the radiometer calibration [2].

The brightness temperature increase was from 0.2 dB to 1.5 dB for various solid fuels used in the experiment. No dependency of the used frequency in the range of chosen band was observed. Also the brightness temperature differences are more important than the absolute value of temperature so the calibration of the radiometer is not essential in this application.

AIMS OF THE DOCTORAL THESIS

The doctoral thesis is focused on new techniques and methods of microwave radiometric remote sensing. Since there are a lot of atmospheric and environmental effects that can decrease reliability of newly planned wireless links or sensors (either microwave or optical) and following recent advances in radiometer technology (e.g. miniaturized MEMS based radiometers which allow to construct small and cheap radiometric devices), new algorithms for undesirable effects detection and prediction have to be proposed.

I The work will be primary focused on derivation of methodologies for prediction and detection of dynamic atmospheric changes relating to rains. In order to get statistically significant amount of measured data a measuring campaign will be accomplished – a 10GHz radiometer was deployed on the roof of FEE in CTU campus. Specific atmospheric effects, e.g. cloudiness and precipitation, will be analyzed based on up to 18 months data samples of brightness temperatures and new dependencies of brightness temperature will be published. A methodology to predict and detect rain events and clouds will be proposed and verified.

II Each summer thousands of square kilometers of forests are burned out with huge impact on both environment and economy. Precise detection and localization of fires is a contemporary well demanded service in order to secure human lives and assets. In order to improve the detection and localization of fires, microwave radiometers can be used for the ground scanning. In comparison of radiometer with IR camera the microwave instrumentation brings the advantage to sense even through obstacles or smoke. In the second aim of the thesis the detectability of a particular fire types by aerial microwave radiometer is investigated with respect to specific parameters like the fire size, temperature and especially radiometer sensitivity. There are several paper published about the fire sensing topic but mainly focused on hardware development and not on methodologies of measurement approaches and data processing. Several measurements will be performed in order to study the fire from radiometric point of view and a new methodology will be described.

WORKING METHODS: Atmosphere Sensing

Measurement Site

In order to validate brightness temperature changes and to obtain better statistical insight, an experimental study was set up in the university campus of the Faculty of Electrical Engineering, Czech Technical University in Prague (CTU), Czech Republic. The experimental measuring system consists of a ground based radiometric station and a set of weather sensors located at two meteorological stations.

The microwave radiometer based on the Dicke switch design [19] was utilized for long-term monitoring of brightness temperature. Using the band at frequencies lower than 37 GHz leads to measurements of the brightness temperature that respond more to rain or cloud liquid emissions. The lower working frequency range of 10.95 - 12.75 GHz (satellite band) was chosen to measure the thermal deviation for two main reasons - we wanted to avoid the strong absorption line of water vapor in the atmosphere at 22 GHz, which would cause partial biasing of measurement results, and secondly because of the availability of technology for satellite receivers. When using band with frequencies higher than 37 GHz, brightness temperature mainly responds to cloud ice scattering [17].

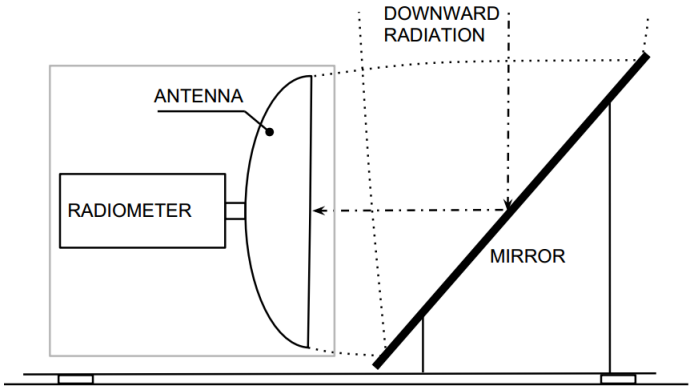

Figure 3: Schematic view on the measurement site.

The vertically pointed radiometer was deployed on the roof of the CTU building, 36 m above the ground level, therefore it was well isolated with respect to the brightness temperature contribution in a given antenna (receiving) radiation pattern of received noise signal from adjacent buildings. The radiometer exterior and internal deployments are shown in Fig. 3 and **??** - the parabolic antenna of the radiometer points towards a tilted planar mirror. As a receiving antenna the parabolic reflector antenna with the diameter of 64 cm was used.

This arrangement was chosen in order to avoid antenna aperture aggradations by any impurities that could affect signal measuring. The metal mirror was also smeared with a hydrophobic film of silicon oil in order to trickle water drops away. The chosen arrangement allows a pure vertical distribution of the ice and liquid content of clouds to be obtained and analyzed.

Table 1: Radiometric system parameters.

Parameter	Value
Radiometer bandwidth	1.7 GHz
Integration time	0.5 ms
Radiometer sensitivity	1.4 K
Antenna beamwidth (-3 dB)	4.4 deg
Sidelobe suppression	>20 dB
Switching frequency	1 kHz
Measuring data averaging interval (all cycles in this period are averaged)	3 s
GPS location	50.10339, 14.392749

Data from two (primary and backup) meteorological stations WS981, made by the Anemo Corporation, Czech Republic [21], have been used for further analysis. Each station collects the temperature and humidity, as well as atmospheric pressure (barometer TMAG 518N4F with range 800 - 1200 hPa), precipitations (heated tipping-bucket rain gauge with a collecting area of 500 cm^2, and the rain amount per one tip of 0.1 mm), and the speed and direction of the wind (anemometer AN 955C). The primary meteorological station is located at same place as the radiometer, i.e. 36 m above ground level. Measurement data are collected in 1 minute intervals, therefore to harmonize the sampling of meteorological and radiometer data, the 3 second intervals of radiometer data were averaged over 1 minute. Only measurements of temperature and precipitation were used for direct processing.

RESULTS: Atmosphere Sensing

Method for Precipitation Prediction

In this section, the relation between measured brightness temperature and weather conditions will be discussed.

Measured data were analyzed over the period of 14 months, from March 2010 to April 2011. During this period 314 clearly defined atmospheric states were observed. These states can be detected or predicted by a microwave radiometer with the use of the proper statistical tools. To achieve the best results the method with variance enumeration was proposed.

The main aim of the paper is to introduce the detection of dynamic atmospheric events that are connected with certain atmospheric states. Initially, the utilization of a microwave radiometer as a precipitation detector and especially for precipitation prediction was investigated.

A simple approach using a steady threshold to predict rain events [6] was dismissed at the beginning of analysis because it had led to a higher number of "False alarms". In Fig. 4 a typical situation is depicted on the set of precipitation and brightness temperature data. In this simple (generally used) steady threshold method of cloud or rain event detection, a particular threshold is first carefully determined. When the brightness temperature exceeds the threshold limit, an event is predicted (Hit indication). The main problem arises with the threshold determination. When a low threshold is chosen to achieve extremely sensitive forecasting (i.e. for radiometer measurements in time intervals shorter than 1 minute), a number of "False alarm" signals are usually generated. By establishing a higher threshold we can on the one hand rapidly reduce the number of false alarms, but on the other hand, as it was confirmed by our analyses, this causes more "Misses" and, what is more, it inconveniently shortens the forecasting period before events. In other words, in many cases it results in the degradation of forecasting information. An example of false alarm signals observed on 24th May 2010 before 12.00 (note: all measurement records are related to UTC) can be distinguished in Fig. 4. In this case, the threshold was set to a value of 80 K of brightness temperature.

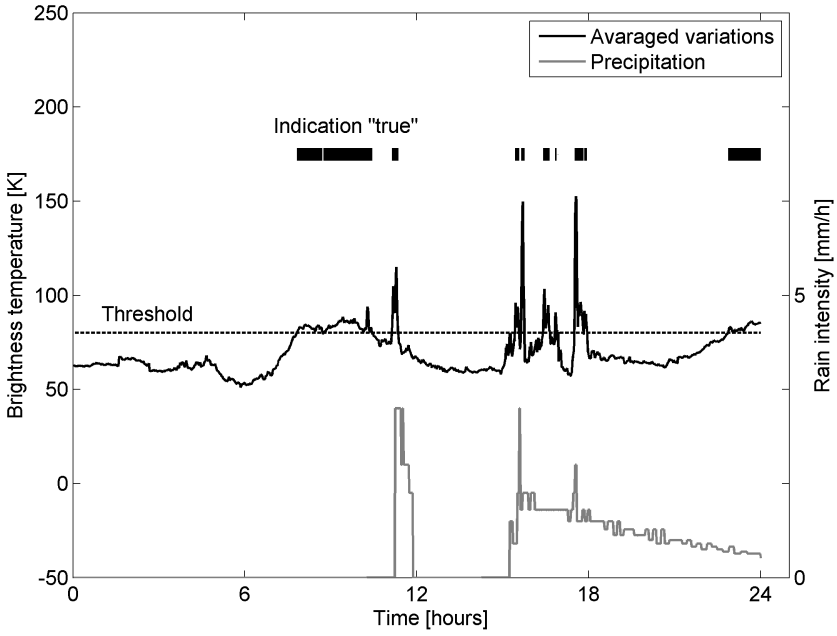

Figure 4: Example of simple threshold method utilization for the prediction of rain events; data from 24th of May 2010.

Since the success rate of the method analyzed above had not proved satisfactory, a more reliable detecting method based on observations that the rapid increase of brightness temperature precedes

rain events was proposed. The new method inheres in brightness temperature variances calculated over a particular time window within the measuring period. By parametric study, a 5 minute window of variance calculation was found to be the most effective. A shorter window results in higher variances even for non-significant events e.g. an artificial ripple in the brightness temperature, while with a longer window the forecasting information degrades or is lost. The same situation as in Fig. 4 is newly demonstrated in Fig. 5, where the threshold was applied to the curve obtained by moving-averaged variances. It can clearly be seen that false alarm signals were suppressed, and only real rain events could be detected in advance without a significant number of false signals.

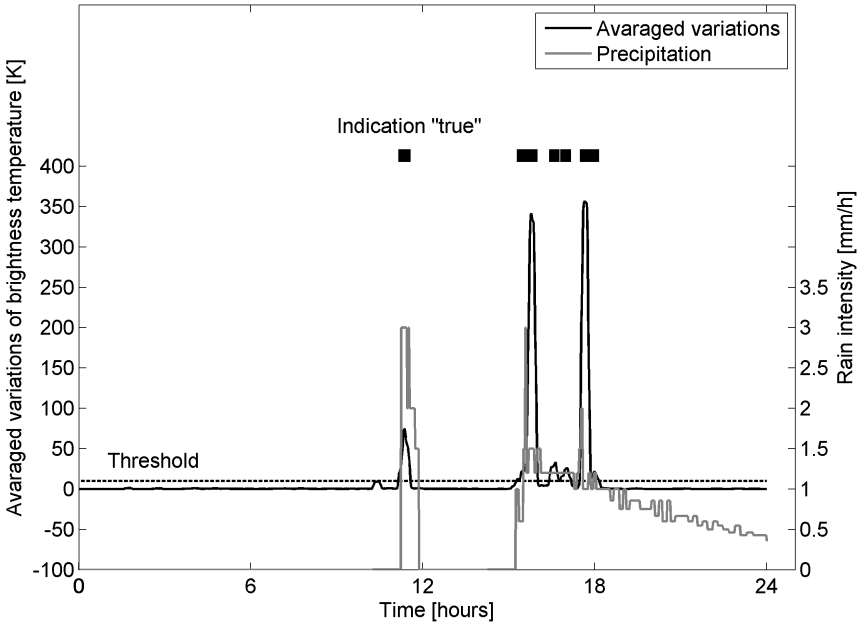

Figure 5: Example of undesirable signals suppression and rain prediction by using the method proposed in this contribution; data from 24th May 2010.

The probability of the successful utilization (hit rate) of the proposed method applied to the whole data set (314 events were considered) is summarized in Tab. 2. The whole range of temperature variations thresholds was scanned and the optimum of 10 K was determined as the value corresponding to the highest and the most stable hit rate over the evaluated period.

Table 2: Hit rate of precipitation forecasting by the proposed method.

Threshold	Event Forecast		
	Yes		No
	Event Observation		Event Observation
	Yes	No	Yes
8 K	75,4 %	11,7 %	12,9 %
9 K	75,1 %	11,4 %	13,6 %
10 K	74,4 %	7,7 %	17,9 %
11 K	70,1 %	7,5 %	22,4 %
12 K	59,5 %	7,3 %	33,2 %

To determine the average forecasting time before rain detection at ground level (note this can be for short intervals more precisely expressed as a detection time), a cross-correlation function was used. Every pattern of events was correlated to the function processed for forecasting (variation, averaging) and the correlation was calculated for different time shifts. The maximum of the cross-correlation product and corresponding forecasting time was derived (see Fig. 6). The average time of

the event forecast before the start of precipitation is 1.8 minutes. Since the variance is calculated over a moving time window of measured data, the result of averaging is delayed to brightness temperature changes. Note that the real peaks of brightness temperature can be observed quite some time before the start of rain (approximately 5 – 10 minutes). The forecasting time of 1.8 minutes represents a compromise value and corresponds to an acceptable number of Hits and False alarms. There is also a certain degree of freedom, and therefore it is possible to choose between a relatively improved forecasting time, but at the cost of a higher number of False alarms or Missed events. The forecasting time is shortened because of the averaging.

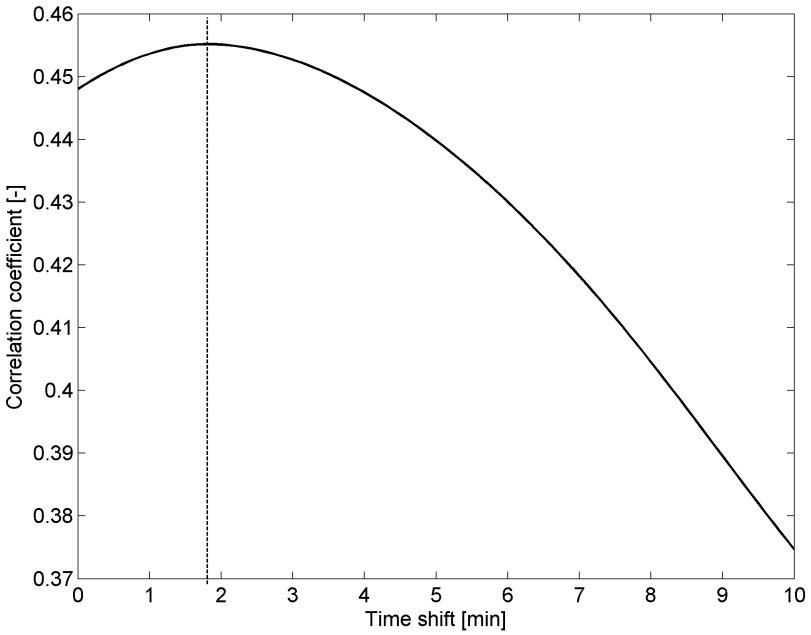

Figure 6: Averaged cross-correlation products of all rain events.

Method for Cloud Detection

Next the cloudiness detection method will be described. After eliminating the influence of rain, brightness temperature measured by the microwave radiometer and meteorological data was further analyzed. Despite a high randomness rate in the meteorological data, some particularly interesting relationships were observed. At first, the brightness temperature varied from 47 K up to 65 K, even during periods of clear skies. The amplitude of the measured brightness temperature was dependent on sunshine, i.e. in the daytime. Almost all the higher brightness temperatures with more rapid brightness temperature changes were related to specific types of cloudiness [18] (for cloudiness types see [27]). These issues were also partially described by Long in [13].

For cloudiness detection, a similar technique was used as for precipitation prediction. This method exploits the instability of brightness temperature when a cloud moves through the observed volume. Again, the variance of the brightness temperature was calculated within a 5minute time window over the entire period.

A typical behavior pattern for brightness temperature is depicted in Fig. 7, where the clouds presence in the monitored volume of atmosphere from 7.00 to 18.00 caused higher variations of the brightness temperature.

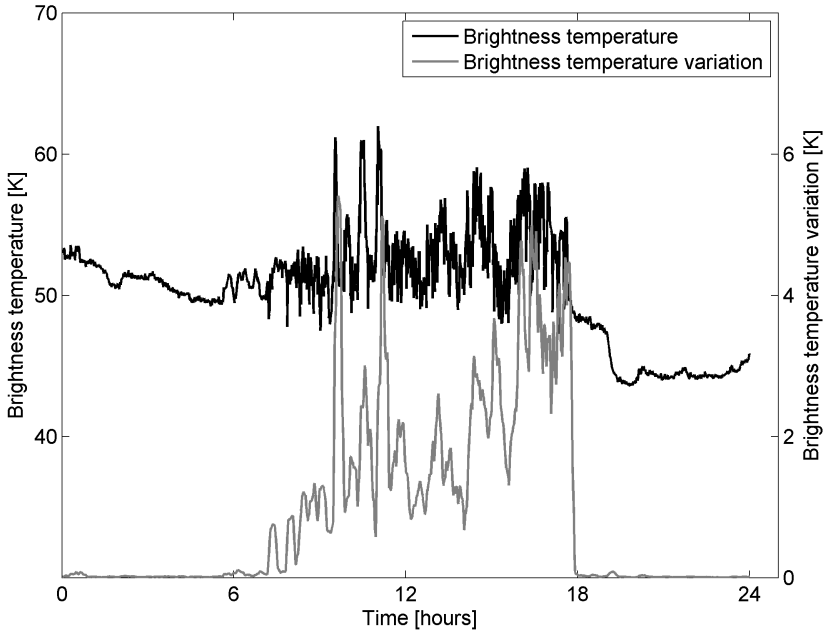

Figure 7: Typical variations of the brightness temperature during clouds presence in the monitored volume of atmosphere on 5th April 2010.

Variations of brightness temperature are depicted as a function of ambient temperature in Fig. 8 (156 events were captured). The incidence of low temperature can be observed. From the measurements it was found that when the ambient temperature is above 0 °C, the variation of brightness temperature due to the cloud presence is higher - in the range from 0.2 to 4 K. It should be emphasized that when the ambient temperature is below 0 °C, the variation ranges from 0 to 0.5 K. The temperature at ground level (measured by the weather station) is highly correlated to the temperature in the monitored volume of atmosphere above (obtained from the radiometer). Since the radiometer is thermally stabilized, possible slow and minor temperature deviations cannot significantly affect the measurements. To ensure correct interpretation of the results, the influence of temperature (below/above 0) is considered and the results are described for both temperature ranges.

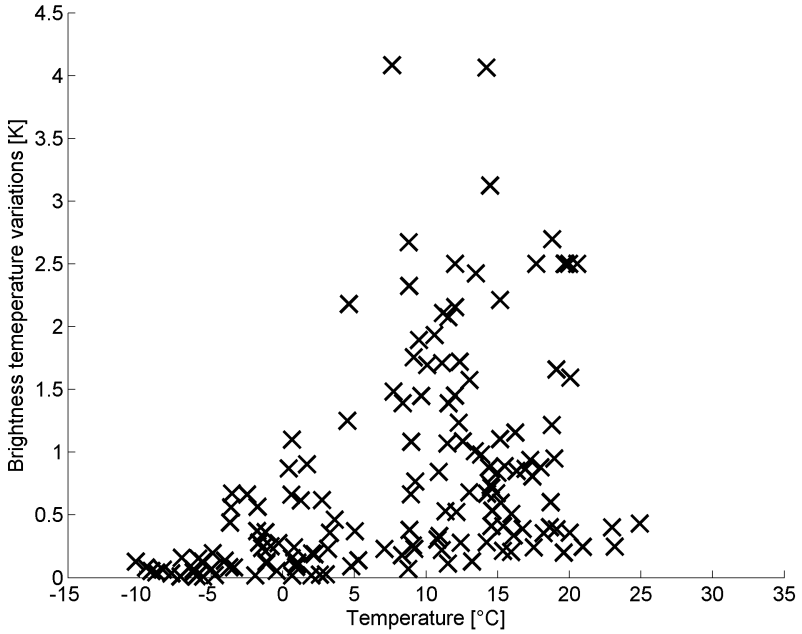

Figure 8: Brightness temperature variations when clouds passed through the vertical volume monitored by the radiometer.

In Fig. 9, variation of brightness temperature is shown in a situation without clouds in the monitored volume of atmosphere – 158 events were captured during the cloudless period. The contrast with the cloudy case (Fig. 8) is obvious. The variation does not exceed the value of 0.25 K during the cloudless period. Variations, based on measurements when clouds were in the observed volume, can be clearly separated from the state when no clouds were present in the observed volume, and hence a method to detect cloudiness based on the calculation of variations can be proposed.

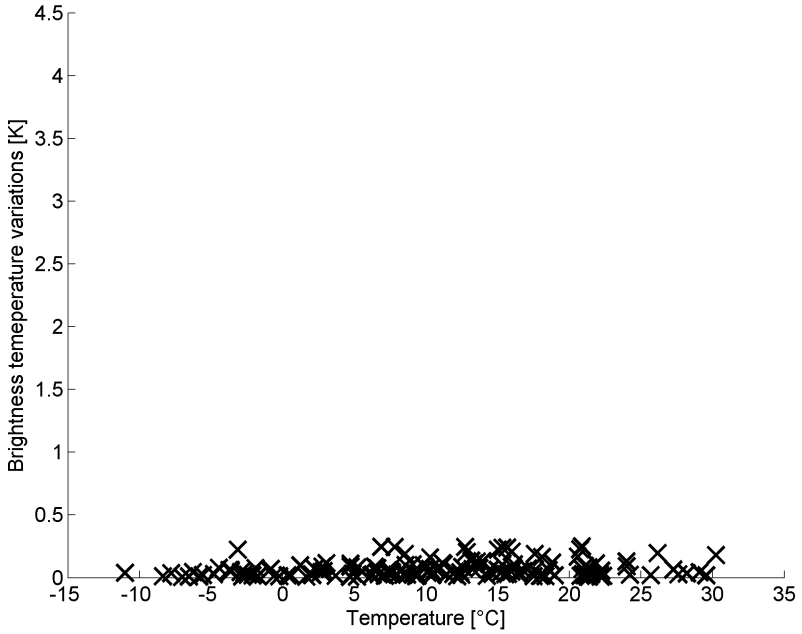

Figure 9: Brightness temperature variations when no clouds were present in the monitored volume of atmosphere.

The threshold of brightness temperature variations for the determination of cloud presence was parametrically determined as 0.23 K. Using this value as a decision-making parameter, the following results listed in Tab. 3 for temperatures higher than 0 °C were obtained from an analysis of 14 months of measurement data (314 captured events). The hit rate of estimates is substantially higher than the hit rate of estimates calculated for ambient temperature below 0 °C, when the method cannot be properly applied. In such cases the hit rate was only 31.43 %.

Table 3: Hit rate of cloudiness forecasting when the temperature was higher than 0 °C.

		Event forecast	
		Yes	No
Event Observation	Yes	80.5 %	4.8 %
	No	14.7 %	

Conclusion

In the chapter the atmospheric model is described. Many atmospheric dynamical effects were captured and the relation of brightness temperature swell that occurs just before a rain was found out. Based on this brightness temperature swell a new methodology of fire detection was proposed and published. The methodology exploits the signal variance as a statistical parameter which steeply grows in advance of a rain event. Similar approach is used for cloud detection and is described further in section .

WORKING METHODS: Fire Sensing Methodology

Principles of remote sensing of the atmosphere and ground are very well described. The fire-endangered environment is scanned by several means using different frequency bands. The basic observation in the visible light spectrum (450-750 nm) is the most inherent for human beings but has some complications. Just the visible part of fire can be seen and in most cases direct flames can be seen and detected. Such observation can be useless in case of obstacles that covers the area of interest or when the fire is in the smoldering phase and has no apparent fire signs. The last argument can be eliminated by using the thermal scanning (1400nm) but still there is a problem with obstacles. Since the microwave radiation can pass natural obstacles it is the reasonable choice to use microwave band as a next means for scanning.

Theoretical Introduction and Analysis of Fire Sensing

Since the fire remote sensing is necessarily the down-looking application several effects must be taken into account. The ground surface is not an ideal environment in terms of microwaves propagation. There is a lot of obstacles and inhomogeneities. The possible fire that should be detected can be easily overlooked just in the tangle of vegetation, sand, wet and dry soil, etc. Also, the emissivity of the sensed surface must be taken into account. The sky reflection has a minor influence on the measurement but cannot be neglected. The derivation is well described in [22].

A general scenario of a spot sensing is depicted in Fig. 10. In this case no fire is present in the sensed spot.

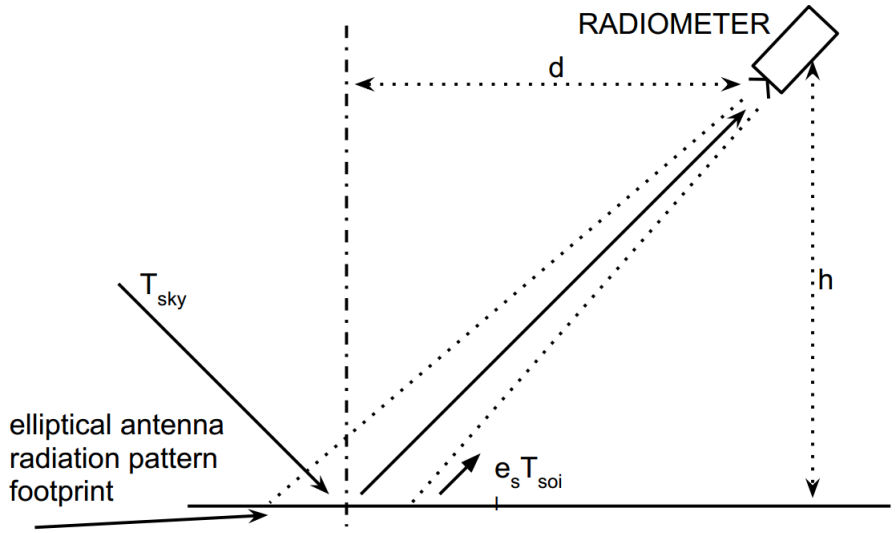

Figure 10: General remote sensing deployment focused on a ground target

The antenna is placed in a particular height h. In this case the sensed temperature consists of two parts - of the soil radiation and from the reflected sky radiation. The part of brightness temperature that comes from soil is weighted by the soil emissivity. Likewise, the downward radiation is weighted by the ground reflectivity.

$$T_A = T_s e_s + (1 - e_s) T_{SKY} \tag{1}$$

Where the T_s stand for the soil thermodynamical temperature, e_s is the emissivity of the soil and the right part of the formula part represents downward radiation T_{SKY} weighted by the soil reflectivity $(1 - e_s)$. The downward radiation consists of the atmospheric emissions and of the cosmic radiation background which is reduced by the atmospheric opacity.

$$T_{SKY} = T_D N + T_{BGD} e^{-\tau_\infty} \tag{2}$$

Soil Emissivity

For early simulations the emissivity described in [16] was used. The emissivity for soil with low vegetation and X band frequency is in the range from 0.92 to 0.95.

First experimental measurement was done in order to obtain the soil emissivity. For this purpose the thermodynamical temperature of soil was measured as well as the brightness temperature of sensed spot and sky brightness temperature. In order to obtain the soil emissivity the formula (3) that comes from formula (**??**) can be used in following expression.

$$e_{soil} = \frac{T_A - T_{SKY}}{T_{soil} - T_{SKY}} \tag{3}$$

During the experiment the radiometer antenna was pointed to the sky under the same elevation angle that was then used for fire sensing but in the upward direction. This measured brightness temperature is the T_{SKY} parameter. Then the antenna was turned to the fire spot (without the fire yet) and the brightness was recorded again. The calculated emissivity is depicted in Fig. 11 during the period of several minutes.

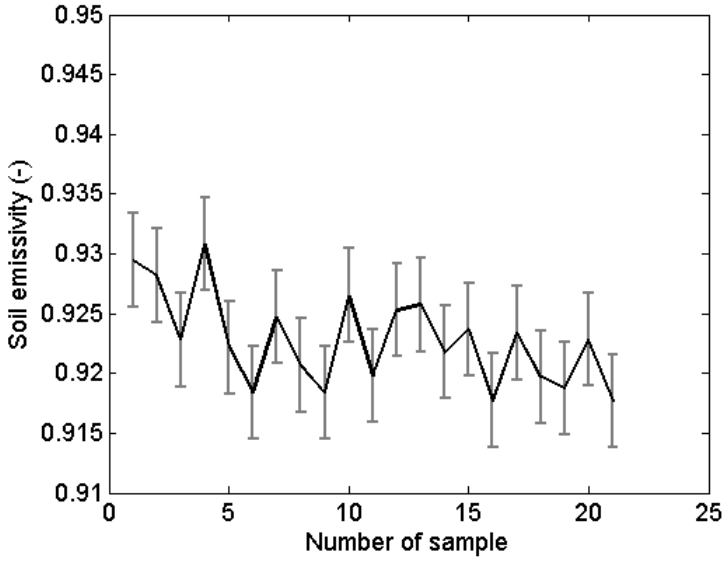

Figure 11: Soil emissivity measurement with marked standard deviation.

The experiment was done during cloudy day when the whole sky was covered by consistent altostratus cloud. The brightness temperature measured when pointing to the sky was in the range of 53 K to 55 K, soil thermodynamical temperature was in the range of 20 to 21 °C (293 – 294 K). Brightness temperature recorded by the radiometer was in the range of 273 to 277 K.

Filling Factor

For the radiometric measurement in relation with sensing of a bounded spot the filling factor quantity is generally used. It is a representative parameter of spatial resolution of the radiometric system. Usually the filling factor is considered as a fraction of the area covered by the fire which is viewed by a radiometer. By using the filling factor the problem with sensing of same fire spot from various distances and under various angles is solved.

Generally the filling factor definition is understood as the power received from a bounded source in relation of the source at the same brightness temperature but filling the whole antenna radiation pattern [9], [8], [20].

Formally the filling factor can be calculated by

$$q = \frac{G_0}{4\pi} \iint\limits_{\Omega_F} P_n(\vartheta, \varphi) d\Omega \tag{4}$$

where G_0 stands for the antenna gain in the direction of maximum radiation, P_n is the normalized radiation pattern and Ω_F means the spatial angle in which the fire spot is visible by the antenna.

For most cases the simple expression of filling factor can be used

$$q = \frac{A_{fire}}{A_{ant}} \tag{5}$$

where A_{fire} stands for the are of fire and the A_{ant} is the antenna radiation pattern footprint restricted by the half-power beam-width.

Fire Emissivity

In order to supplement general knowledge about the fire sensing, the fire emissivity can be found. When using approach by [14] the radiometric contrast of a fire spot and bare soil can be defined as

$$\rho_T = \tau_{veg}\tau_{atm}[e_{fire}T_{fire} - e_{soil}T_{soil} - (e_{fire} - e_{soil})e_{veg}T_{veg}]q \tag{6}$$

where τ_{veg} is the transmissivity of vegetation that can cover the fire spot, τ_{atm} is the transmissivity of atmosphere, e_{fire}, e_{soil}, e_{veg} stands for the fire emissivity, soil and vegetation respectively. T_{fire}, T_{soil} and T_{veg} are the thermodynamical temperatures of corresponding objects.

Considering that no vegetation was over the fire spot and transmissivity of atmosphere of 1 the relation 6 can be simplified as

$$\rho_T = (e_{fire}T_{fire} - e_{soil}T_{soil})q \tag{7}$$

and the fire emissivity can be expressed as

$$e_{fire} = \frac{\frac{\rho_T}{q} + e_{soil}T_{soil}}{T_{fire}} \tag{8}$$

Since the soil emissivity can be measured as well as the soil and fire temperature the fire emissivity is an accessible number. In chapters – this relation is used for emissivity calculation. Also all scenarios were numerically simulated in MATLAB where the thermodynamical temperature of all objects, known emissivities and environmental parameters were taken into account. The simulation result is mentioned in following chapters as well.

RESULTS: Fire Sensing Methodology

Fire Detectability

In the chapter the detectability of a fire by a microwave radiometer is investigated. Simulations of several scenarios and together with outdoor measurement were performed in order to confirm detectability of the fire of specific temperature distributions and dimensions. Various scenarios for fire sensing were numerically modeled and simulated. Real parameters of antenna radiation pattern and radiometer sensitivity were taken into account. The concept of fire detectability verification was tested on real measurement data and then applied in a large scale on analyses of scaled airborne sensing of an environment. The results clearly indicate the possibilities and limits of detection with currently available radiometers.

The brightness temperature was calculated in simulations' stage by

$$T_A = \frac{1}{\Omega_A} \oiint_{4\pi} F(\Theta, \varphi)T_B(\Theta, \varphi)d\Omega \tag{9}$$

where T_A is the antenna detected noise temperature, F represents the antenna radiation pattern and T_B stands for the brightness temperature at given azimuth Θ and elevation φ angles.

In the following chapters several types of fires were measured in order to obtain the emissivity of various burning matter.

Airborne Sensing

When the wild fires are monitored it is usually done by a remote sensing, mainly in IR range and experimentally in a microwave band. In both cases the airborne sensing is often used. For the start a feasibility study of fire detectability by airborne sensing was done. The whole scenario was numerically simulated then downscaled to dimensions that are possible to measure in the natural environment by the available measuring system, it was measured and the model was verified. The down scaled scenario is described in next sections.

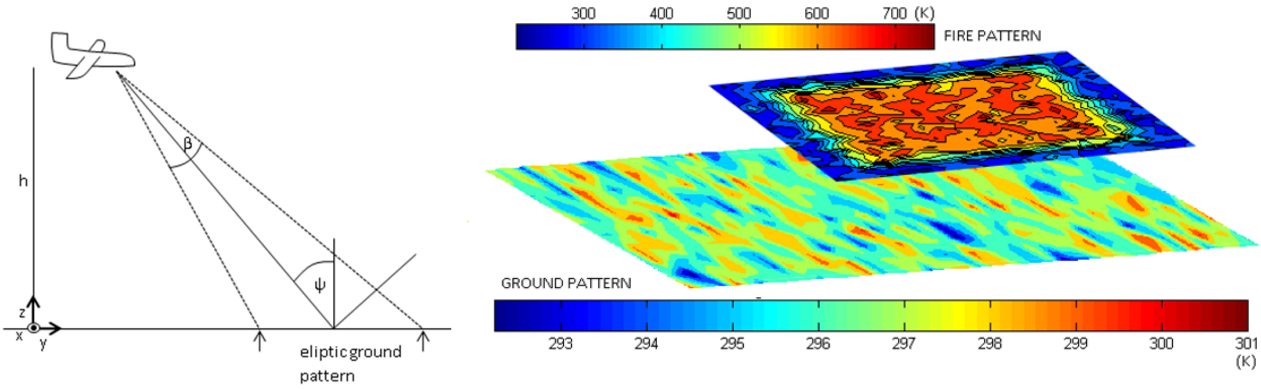

(a) General schematic view.

(b) fire and ground temperature pattern (fire pattern is depicted in reduced scale)

Figure 12: Scenarios schemes

Various scenarios have been analyzed. The typical scanning scene is depicted in the Fig. 12a . Let us assume the ground being sensed by an airborne radiometer at 300 m above ground level (h), with incident angle (Ψ) up to 45° in the forward direction of the track. In that case, the ground area scanned by antenna beam has elliptical pattern. For analyses we assumed the ground plane area 500 m × 2400 m (width × length) with resolution 0.5 m/pixel. The analyzed fire was located from small scales up to 2/3 of the ground plane length.

Numerical analysis of above mentioned scenario was performed in order to define the basic task of airborne sensing. Results from the analysis are shown in Fig. 13 .

The brightness temperature in the simulation was calculated by equation 9.

Several fire types were analyzed. Results in this thesis are based on simulation of the fire TF1 standardized in EN54, Part 9 [15].

Fire in the first smoldering stage having the temperature in the range 220 to 290 °C was assumed [26]. In this analysis 3 radiometers were considered: i) state-of-the-art radiometer [3], ii) commercially available radiometer [12], and iii) radiometer from our laboratory [4]. Main results of the analysis represent the fire dimensions that are still detectable with the mentioned instruments.

The results from analysis – the limits in microwave radiometer detection of fire – is shown in Table 4. Three values of radiometer sensitivity were used to verify detectability of the fire. The first one is for case of the state of the art radiometer with sensitivity 0.1 K [[3]], the second one for the commercially available radiometer [9] having sensitivity of 0.7 K and the third one representing the Dicke-type radiometer available in our laboratory with sensitivity of 1.2 K [4].

Table 4: Detectable fires sizes with respect to radiometer sensitivity.

			Event forecast		
Dimensions of fire (m × m)	Temperature of fire (°C)	Brightness temperature contrast (K)	State-of-art radiometer	Commercial radiometer	Radiometer at CTU lab
4.5 × 4.5	220-290	0.11	YES	NO	NO
10 × 10	220-290	0.72	YES	YES	NO
13 × 13	220-290	1.23	YES	YES	YES
4 × 4	300-350	0.13	YES	NO	NO
9.5 × 9.5	300-350	0.71	YES	YES	NO
11 × 1	300-350	1.35	YES	YES	YES

In the Fig. 13 is the example of sensed brightness temperature contrast that is detectable by above mentioned radiometers.

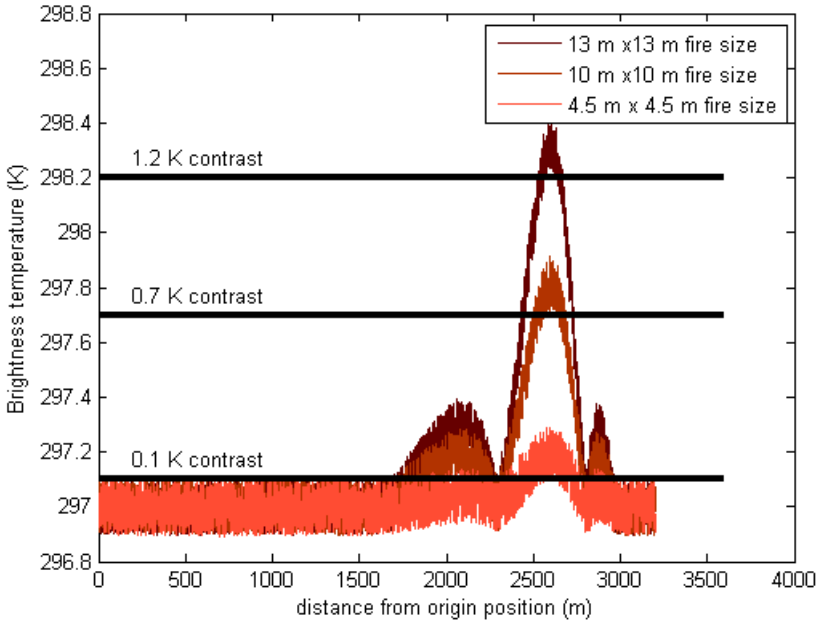

Figure 13: Three fires with different size at the temperature in the range of 220 - 290 °C.

The influence of the fire area brightness temperature distribution was considered as well as various ground plane temperature distribution. Derived results can help hardware designers of radiometric instruments to design a receiver for the purpose of fire sensing with properly set sensitivity with respect to other radiometer potentially adjustable parameters (integration time).

Simulation of the above described scenario was done at first, and then it was verified by the measurement.

Gasoline Fire

Next fire was the gasoline fire. It was used 100 cc of gasoline to be absorbed into a cotton fabric. Size of the fabric was 50 × 50 cm. By the fabric it is preserved the fire size, shape and homogeneous gasoline distribution in the sensed area. Time of the whole measurement was approximately 11 minutes. In Figure 14 the course of the burning is depicted in series of 4 pictures.

Figure 14: Burning of the gasoline fire in 4-picture time series. Fire size 50 × 50 cm.

In Figure 15 the measured brightness temperature in a time series is depicted. The ignition occurred in 7th minute and the whole combustion took approximately 2 minutes.

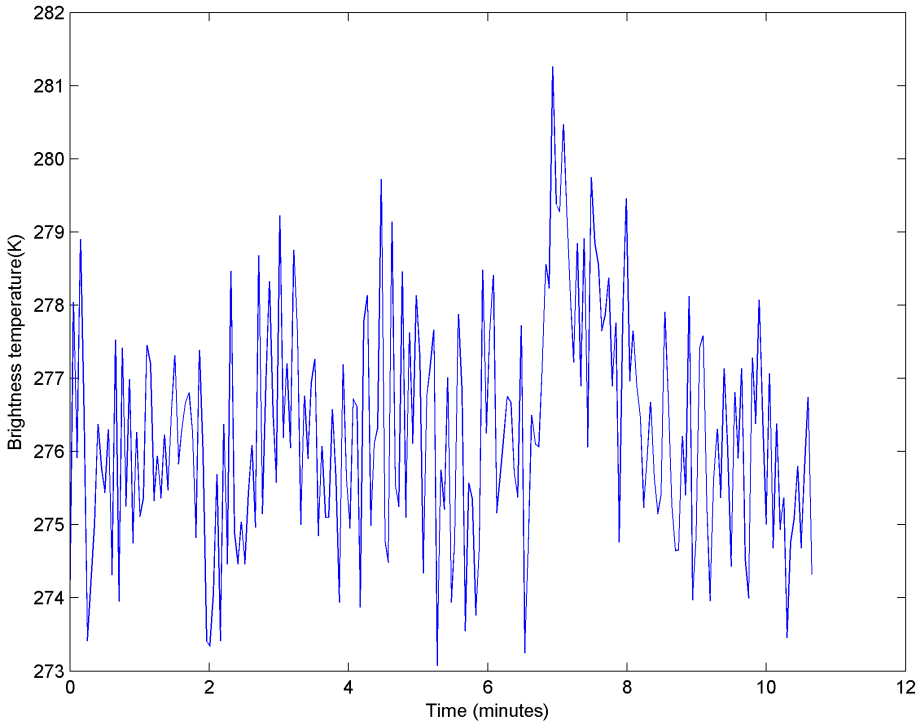

Figure 15: Gasoline fire microwave signature. Fire size 50 × 50 cm.

From the know parameters the fire place emissivity, the filling factor and other parameters can be calculated. List of measured and calculated values is in Table 5.

Table 5: Gasoline fire measured parameters.

Parameter	Value
$T_{ant,soil}$	276.1 K
$T_{ant,fire}$	280.2 K
T_{soil}	294 K
T_{fire}	∼1220 K
$T_{contrast}$	4.1 K
$e_{fire,sim}$	0.247
e_{soil}	0.92
$e_{fire,meas}$	0.248
q	13.9 %

Where $T_{ant,fire}$ is the averaged maximum brightness temperature measured during the burning process, $e_{fire,sim}$ stands for the fire emissivity that was numerically simulated and $e_{fire,meas}$ means the fire emissivity that was calculated from measurement by 8.

Flood Trash Fire

For the measurement the flood trash fire was chosen. It was used 1kg of the flood trash that consists of dry grass, wood, dust and wooden bark. Size of the fire was 50 × 50 cm. The material was evenly spread over the spot. Time of the whole measurement was approximately 13 minutes but the burning itself took approximately 5 minutes.

In Figure 16 the measured brightness temperature in a time series is depicted. The ignition occurred in 5th minute. Since the flood trash was still wet just the smoldering stage of the fire occurred.

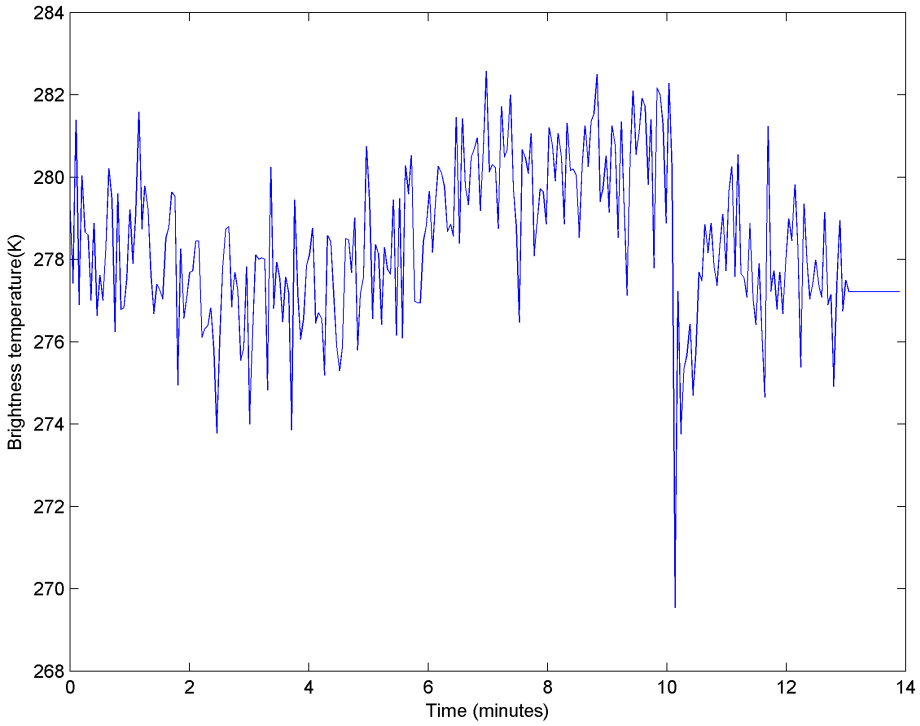

Figure 16: Flood trash fire microwave signature. Size 50 × 50 cm.

The signal drop that occurred after 10th minute was caused by removing the rest of smoldering material with a metal tools.

From the know parameters the fire place emissivity, the filling factor and other parameters can be calculated. List of measured and calculated values is in Table 6.

Table 6: Flood trash fire measured parameters.

Parameter	Value
$T_{ant,soil}$	277 K
$T_{ant,fire}$	280.4 K
T_{soil}	294 K
T_{fire}	∼1150 K
$T_{contrast}$	3.4 K
$e_{fire,sim}$	0.256
e_{soil}	0.93
$e_{fire,meas}$	0.257
q	13.9 %

Wood Fire

The ignition of wood fire occurred in 6th minute – the first signal drop is apparent and it is caused by a worker who started the fire. Next, the fire was twice checked – the drop in 8th minute and 10th minute, caused again by a worker.

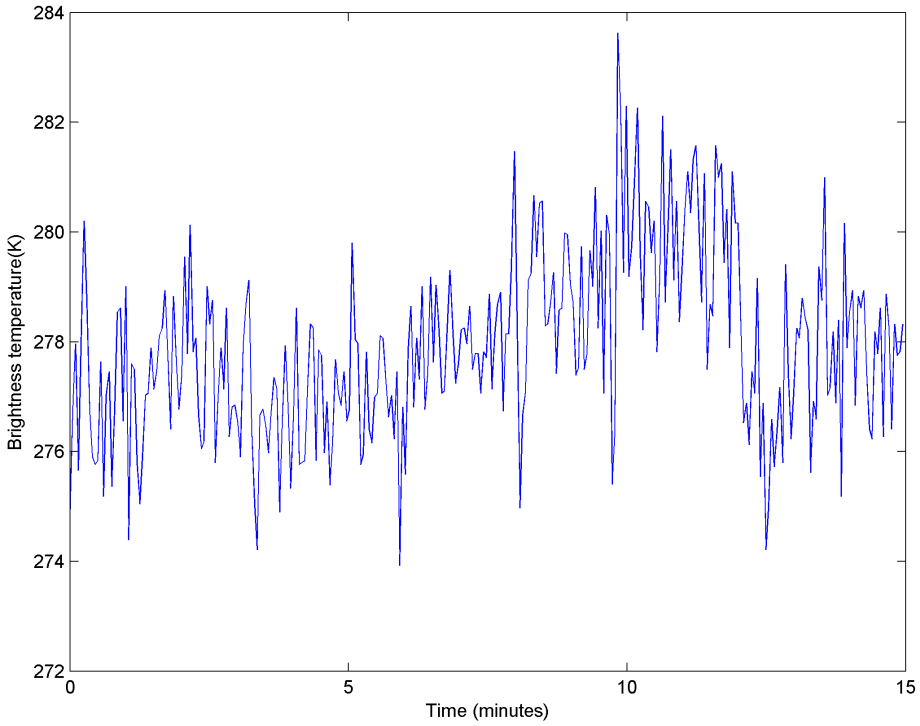

Figure 17: Wood fire microwave signature. Fire size 50 × 50 cm.

From the know parameters fire place emissivity, the filling factor and other parameters can be calculated. List of measured and calculated values is in Table 7.

Table 7: Wood fire measured parameters.

Parameter	Value
$T_{ant,soil}$	277.1 K
$T_{ant,fire}$	281.1 K
T_{soil}	294 K
T_{fire}	∼1200 K
$T_{contrast}$	4 K
$e_{fire,sim}$	0.252
e_{soil}	0.93
$e_{fire,meas}$	0.257
q	13.9 %

Straw Fire

In order to measure a well burning material with rapid ignition the straw fire were recorded. Those fires were measured also with bigger fire spot in order to measure with various filling factor.

Since the straw burns very rapidly a clear brightness temperature signature was recorded. Maximum brightness temperature was 290.1 K (averaging several top values). Ignition started at 5th minute and the whole burning took approximately 3 minutes.

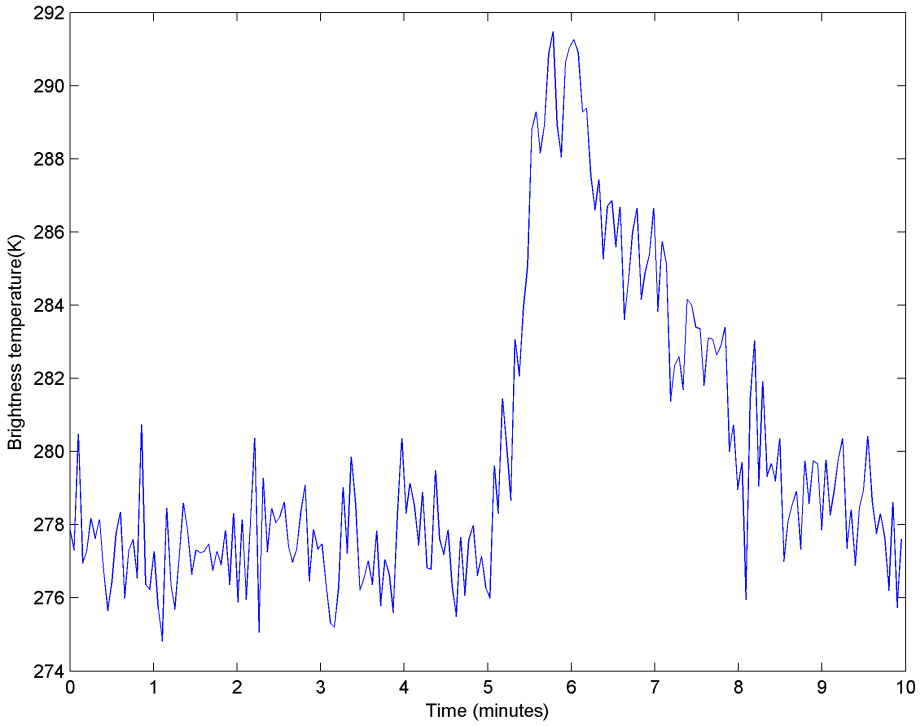

Figure 18: Straw fire microwave signature. Fire size 50 × 50 cm.

All measured values and parameters of the first straw fire are listed in Table 8.

Table 8: Straw fire measured parameters. Fire size 50 × 50 cm.

Parameter	Value
$T_{ant,soil}$	277.2 K
$T_{ant,fire}$	290.1 K
T_{soil}	294 K
T_{fire}	∼1420 K
$T_{contrast}$	12.9 K
$e_{fire,sim}$	0.254
e_{soil}	0.93
$e_{fire,meas}$	0.250
q	13.9 %

Fire Size and Temperature Influence

For the remote sensing of fire the influence of the fire size on the detectability is necessary to find out as well as the fire temperature influence. The methodology of fire sensing is based on the different radiometric contrast caused by various fire temperature, size, emissivity of the places that are supposed to be sensed. In the following simulations and measurement both was investigated.

The same radiometric system as is described in chapter was used but the deployment of the radiometer and measured spot was different.

For comparison purposes, an additional 2D-thermal fire sensing and scanning of surrounding temperature distribution was done by the FLIR i7 infrared camera [7].

A general scenario of simulations and measurement by the radiometer is depicted in Fig. 19. Such setup introduces typically used deployment for airborne sensing [25] so it is a good approximation of the up-scaled scenario. During the outdoor measurement the radiometer was placed in the height of

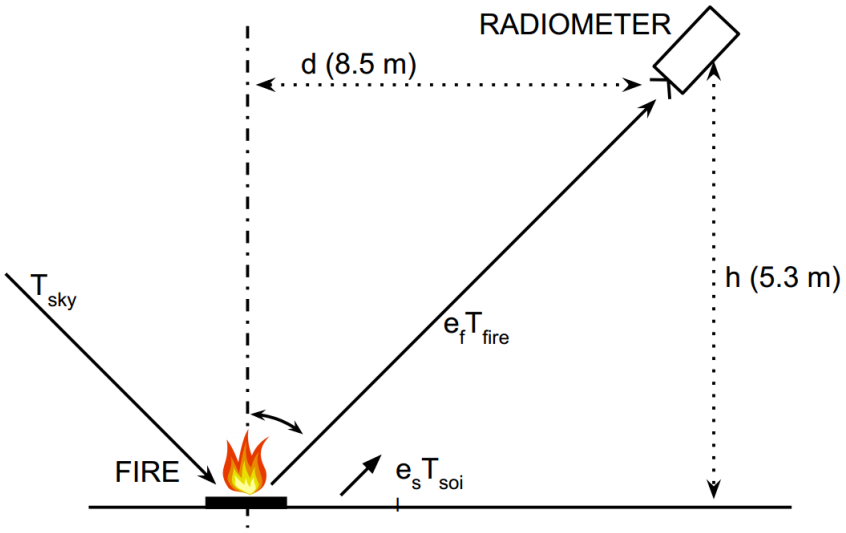

Figure 19: Fire measurement deployment.

5.3 meters. The incident angle (Ψ) was 62°. Antenna was pointed to the center of fire area. The filling factor [22] in this case was about 15 %.

The same situation was numerically analyzed and the analogical numerical model was designed having resolution of 1 cm. The whole scenario was discretized and contribution of each cell to the total brightness temperature was taken into account. Every cell had a specific temperature and the antenna radiation pattern was involved in the simulation as well.

Fire size varied from the square area of 0.3 m × 0.3 m to 0.7 m × 0.7 m. Fire temperature varied in the range of 500 °C to approx. 1200 °C (due to the lower dynamic range of IR camera the upper temperature range was approximated).

Before the start of the first outdoor fire measurement, the brightness temperature background was sensed. The measured ground area had temperature distribution in the range of 5 to 15 °C. The soil was dry after a sunny day covered with grass. Figure 20 depicts sample of time series of measured and simulated data of brightness temperatures. The conditions of measurement were very steady, the brightness temperature of the background was stable more then 30 minutes.

For the first scenario a constant fire size was assumed and various temperatures were considered. The fire area had approximately square shape covering the size of 50 × 50 cm. The fire activated from glowing wooden sticks reached highs up to 2 m high having bright flames with the temperature approx. up to 1200 °C [15]. Fire development in time as caught by 4 IR shot sequences in 7 minutes is depicted in Figure 21 .

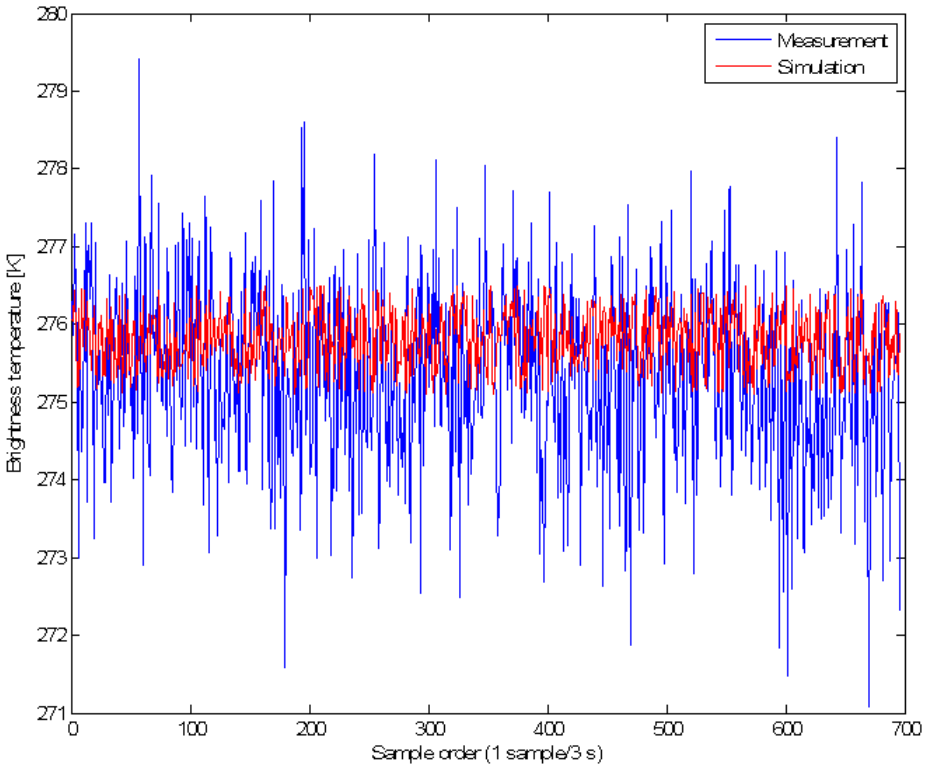

Figure 20: Measured background brightness temperature.

Figure 21: Fire development captured by the thermo-camera, temperature range is estimated up to approx. 1200 °C.

Recorded brightness temperature with dependence on fire temperature is in Figure 22.

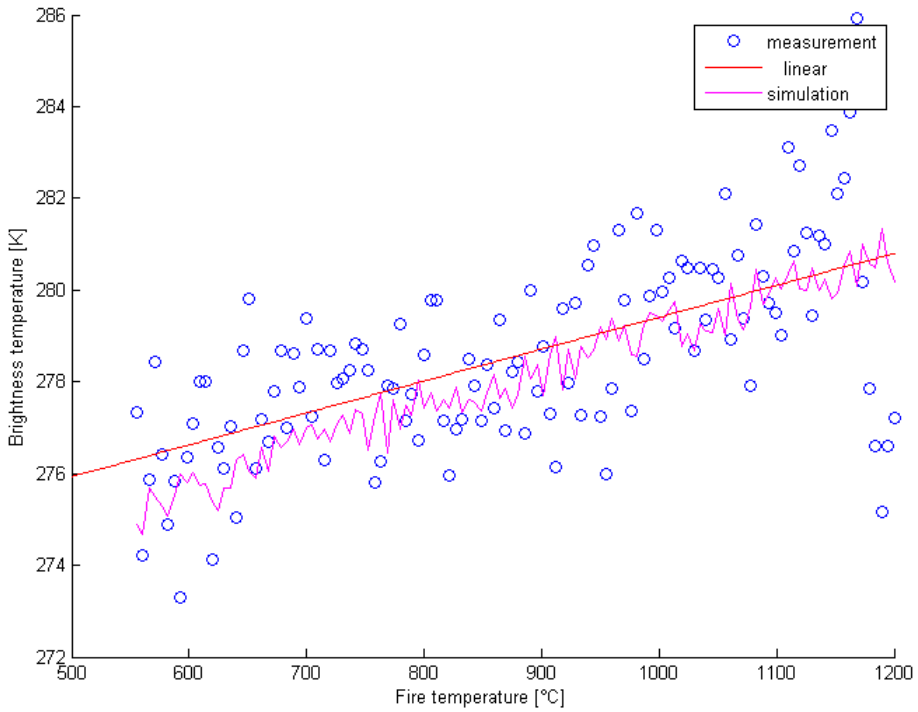

Figure 22: Measured brightness temperature as a dependency on fire temperature.

The fire temperature was activated by a compressed air and checked by the IR camera. Unfortunately, the low dynamical range of the available camera couldn't provide accurate values of the temperature so in later stages the temperature was estimated.

Second measurement was performed to capture brightness temperature as a dependency on fire size. The fire had a square shape varying from the size 0.3 m $\times$ 0.3 m to 0.7 m $\times$ 0.7 m. Temperature of the fire constant and was in the range of 500 to 600 °C. For this measurement only glowing charcoals were used in order to easily manipulate with the hot material. Measured values are shown in Figure 23.

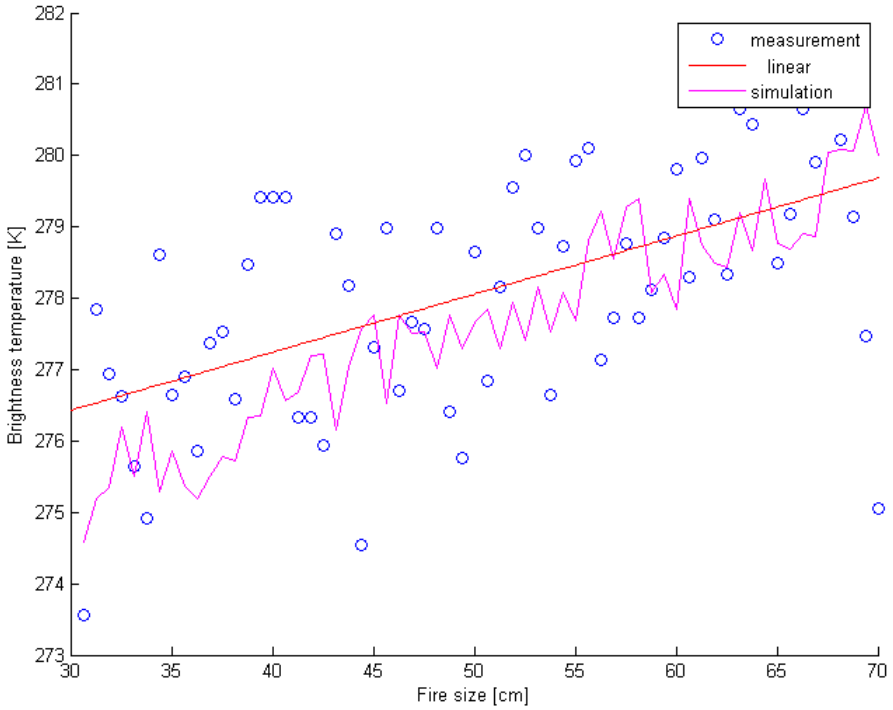

Figure 23: Measured brightness temperature as a function of fire size (x-axis describes length of edge of the square fire area).

In this case the resolution of numerical model was set to 10 cm per pixel (the smallest fire pixel size was assumed to be 10 × 10 cm). In the first approach, the model of fire had set constant temperature 550 °C (for distances and deployment see section the picture of deployment above). Results of analysis in terms of the dependency of fire size on brightness temperature contrast are described in Table 9.

Table 9: Dependency of demanded radiometer sensitivity on the fire size to be detected.

Fire temperature (°C)	Fire dimensions (cm)	Brightness temperature contrast (K)
550	10 × 10	0.17
550	20 × 20	0.69
550	50 × 50	4.29
550	100 × 100	16.76

Let us assume the ground without a fire has homogeneous temperature distribution. Once the lobe of antenna scans the fire area, the brightness temperature swell is recorded. Table 9 then distinguishes which fire size is detectable by specified brightness temperature contrast. For instance the brightness temperature contrast of fire having size of 10 × 10 cm is approximately 0.17 K. So the minimal radiometer sensitivity for detection such fire has to be at least 0.17 K as well. Next simulated scenario was analyzed to obtain the dependence for possibly measured contrasts of brightness temperatures under various fire temperatures. In this case the fire was set constant with size of 50 cm × 50 cm. The corresponding results of analysis are depicted in Table 10.

Table 10: Dependency of demanded radiometer sensitivity on the fire temperature to be detected.

Fire temperature (°C)	Fire dimensions (cm)	Brightness temperature contrast (K)
550	50 × 50	4.29
600	50 × 50	5.06
800	50 × 50	8.21
1000	50 × 50	11.35

E.g. for the size of mentioned fire with a temperature 550 °C is the brightness temperature contrast approximately 4 K. By the methodology of the fire sensing sensitivity with respect to the fire size it is necessary to involve in measurement a radiometer with the sensitivity of 4 K at least.

Methodology of Fire Sensing

The fire sensing is a complex task and the final measured brightness temperature depends on many effects which should be taken into account. During an on site measurement environmental parameters plays a significant role and must be known as well as the technological constraints of used radiometric system.

In order to sense a possible fire in the field the environmental parameters should be know. As the first step of the methodology the soil properties is necessary to consider. From the radiometric remote sensing point of view it is essential to know the soil emissivity or emissivity of any other natural background. How to measure it is described in chapter . The emissivity can vary from 0.8 to 0.95 and it is different for various vegetation types, sand, soil any other material and also depends on humidity etc.

Once the soil emissivity is known the limiting fire parameters to be detected must be found. In chapter a possible scenarios are listed. Fire sizes and its temperature influence on the detectability by a microwave radiometer are described with the minimal sensitivity which must be used. In Fig. 24 the dependency of fire temperature and its emissivity on the detectable radiometric contrast is depicted.

Radiometer sensitivity is the next parameter which is crucial for radiometric sensing of any objects. When this parameter can be chosen (during the instrumentation development) the choice must be based on the sensitivity study described above and in [5].

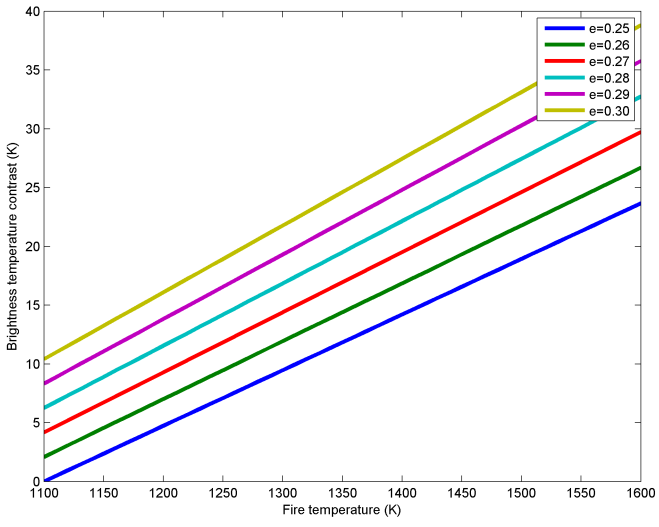

Figure 24: Radiometric contrast as a dependence on fire temperature and fire emissivity.

There are several ways for wild fire detection but the airborne sensing is the most convenient

way in order to cover an extensive area in a short time. The last parameter is necessary to know and to set: filling factor as is described in chapter . The filling factor has significant influence on the possibility of fire detection. From Figure 25 the dependency of filling factor of fire with certain temperature is depicted.

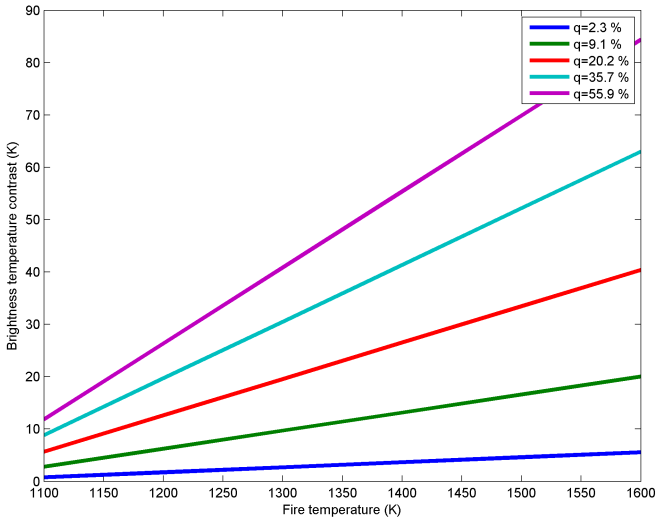

Figure 25: Radiometric contrast as a dependence on fire temperature and the filling factor.

When the radiometric system sensitivity is given and the fire temperature is known or expected it is possible to calculate the filling factor in order to plan e.g. altitude of the radiometer position. In following equation

$$q = \frac{\rho_T}{(e_{fire}T_{fire} - e_{soil}T_{soil})} \tag{10}$$

the ρ_T stands for the demanded brightness temperature or the radiometer sensitivity respectively.

Conclusion

Based on the simulated and measured data the study of microwave radiometer sensitivity was done. Down-scaled scenario of airborne sensing was simulated and measured. The possibilities of fire sensing were investigated. Two cases were measured, fire having different scales either of temperature or being spread on different dimensions. Then, the situation was scaled up and analyzed with the same algorithm for airborne distances and deployment. The output of the study is dependency of brightness temperature contrast on various fire sizes and fire temperatures.

CONCLUSION

The goal of the thesis was to find new methodologies of remote sensing based on microwave radiometer. The dissertation thesis has two fundamental cores. The first one is the new methodology for rain precipitation and cloud now-casting using a microwave radiometer. All the measurements were done in the period of four years and a huge amount of data has been recorded. In the datasets a lot of atmospheric events was recorded and analyzed in order to propose a new methodology how the rain can be fore-casted. For the forecasting of rain the method of detecting the initial brightness temperature swell was used. For the cloud detection methodology the brightness temperature variance was used. Both methodologies are based on measured data, validated by further use of the radiometer and also published in [4].

The second part of the thesis deals with the detection of fires by the microwave radiometer. The requirement and methodology to detect the fire is to be able to find enough brightness temperature contrast. The new methodology of fire detection is based on differences of emissivities of various matters. Since the soil, vegetation, human body and fire has significant difference of microwave emissivity the new methodology can be based on this parameter. Several measurements under natural conditions were performed in order to explore the microwave signatures of various fire types (cellulose, gasoline, straw, trash) and to derive the best possible results. The influence of fire size and temperature on the radiated and measured power was explored and explained.

The result of the thesis are two new methodologies of remote sensing by the microwave radiometer which allows to improve current possibilities of rain prediction, cloud detection. New methodology for fire sensing leads to better protection of human lives and property. The new methodologies open the way for following research that should be done because the substance of the issues is well understood but still there is a lot work to do in order the understand deeper the nature of all the natural effects.

References

[1] P. A. R. Ade and and others. Planck early results: The planck mission. *Astronomy and Astrophysics*, 16464, 2011.

[2] F. Alimenti, T. Kempka, G. Tasselli, S. Bonafoni, P. Basili, L. Roselli, K. Solbach, and H. I. Willms. Fire detection by low-cost microwave radiometric sensors. In *Microwave Radiometry and Remote Sensing of the Environment, 2008. MICRORAD 2008*, pages 1–4.

[3] F. Alimenti, D. Zito, A. Boni, M. Borgarino, A. Fonte, A. Carboni, S. Leone, M. Pifferi, L. Roselli, B. Neri, and R. Menozzi. System-on-chip microwave radiometer for thermal remote sensing and its application to the forest fire detection. In *Electronics, Circuits and Systems, 2008. ICECS 2008. 15th IEEE International Conference on*, pages 1265–1268.

[4] P. Dvorak, M. Mazanek, and S. Zvanovec. Short-term prediction and detection of dynamic atmospheric phenomena by microwave radiometer. 21(4):1060–1066, 2010.

[5] P. Dvorak and S. Zvanovec. On the sensitivity of fire detection by a microwave radiometer. 2013.

[6] R.R. Ferraro, E.A. Smith, W. Berg, and G.J. Huffman. A screening methodology for passive microwave precipitation retrieval algorithms. *Journal of the Atmospheric Sciences*, 55(9):1583–1600, 1998.

[7] Inc. FLIR Systems. Flir i-series infrared camera comparison chart. http://www.flir.com/thermography/americas/us/view/?id=54156&collectionid=601&col=54163?, 2013. [Online; accessed 19-June-2013].

[8] P. Goldsmith. *Quasioptical Systems:Gaussian Beam Quasioptical Propogation and Applications*. Wiley-IEEE Press.

[9] P.F. Goldsmith, C.-T. Hsieh, G.R. Huguenin, J. Kapitzky, and E.L. Moore. Focal plane imaging systems for millimeter wavelengths. *Microwave Theory and Techniques, IEEE Transactions on*, 41(10):1664–1675, 1993.

[10] J. Gueldner and D. Spankuch. Results of year-round remotely sensed integrated water vapor by ground-based microwave radiometry. *Journal of Applied Meteorology*, 38:981–988, 1999.

[11] Y. A. Hussin. Modis - moderate resolution imaging spectro-radiometry for forest detection, 6 - 10 Feb 2005 2005.

[12] PopStefanija. I. Airborne l-band radiometers for remote sensing of soil moisture. *Commercial product datasheet*, 2012.

[13] D.G. Long, Q.P. Remund, and D.L. Daum. A cloud-removal algorithm for ssm/i data. *Geoscience and Remote Sensing, IEEE Transactions on*, 37(1):54–62, 1999.

[14] G. Luzzi, P. Ferrazzoli, S. Gagliani, and T. Mazzoni. Microwave radiometry as a tool for forest fire detection: Model analysis and preliminary experiments. pages 411–418.

[15] European Committee of standardization. En 54-9 components of automatic fire detection systems.

[16] S. Paloscia. Contribution of microwave radiometry in agrometeorological studies. 2, 1993.

[17] E. A. Sharkov. *Passive Microwave Remote Sensing of the Earth*. Books in geophysical science. Springer-Verlag, New York, 2009.

[18] G.M. Skofronick-Jackson, A.J. Gasiewski, and J.R. Wang. Influence of microphysical cloud parameterizations on microwave brightness temperatures. *Geoscience and Remote Sensing, IEEE Transactions on*, 40(1):187–196, 2002.

[19] N. Skou and D. Le Vine. *Microwave Radiometer Systems: Design and Analysis*. Artech House, Norwood, 2006.

[20] D. Solimini. *Microwave Radiometry and Remote Sensing of The Environment*. VSP.

[21] Anemo s.r.o. Ws981 (manual), May 2010.

[22] G. Tasselli, F. Alimenti, S. Bonafoni, P. Basili, and L. Roselli. Fire detection by microwave radiometric sensors: Modeling a scenario in the presence of obstacles. *Geoscience and Remote Sensing, IEEE Transactions on*, 48(1):314–324, 2010.

[23] G. Tasselli, F. Alimenti, A. Fonte, D. Zito, L. Roselli, D. De Rossi, A. Lanata, B. Neri, and A. Tognetti. Wearable microwave radiometers for remote fire detection: System-on-chip (soc) design and proof of the concept. In *Engineering in Medicine and Biology Society, 2008. EMBS 2008. 30th Annual International Conference of the IEEE*, pages 981–984.

[24] L. Terenzi. Cryogenic environment and performance for testing the planck radiometers. *Journal of Instrumentation*, 4, 2009.

[25] F. T. Ulaby, R. K. Moore, and A. K. Fung. *Microwave Remote Sensing, Active and Passive*.

[26] Babrauskas. V. Ignition of wood: A review of the state of the art. *Interflam 2001*, 2001.

[27] World Meteorological Organization (WMO). *Guide to Meteorological Instruments and Methods of Observation*. Geneva, 2008.

[28] H. Y. Won, Yeon-Hee Kim, and Hee-Sang Lee. An application of brightness temperature received from a ground-based microwave radiometer to estimation of precipitation occurrences and rainfall intensity. *Asia-Pacific Journal of Atmospheric Sciences*, 45(1):55–69, 2009.

Publikace vztahující se k tématu disertační práce

Publikace v impaktovaných časopisech:

Petr Dvorak (33 %), Milos Mazanek, Stanislav Zvánovec. Short-term Prediction and Detection of Dynamic Atmospheric Phenomena by Microwave Radiometer. Radioengineering. 2012, vol. 21, no. 4, p. 1060-1066. ISSN 1210-2512.
Citováno: bez citace

Publikace v recenzovaných časopisech

Patenty

Petr Dvorak (50 %), Jiri Libich. Diferenciální teplotní senzor. [Funkční vzorek]. 2010.

Publikace excerpované WOS

Petr Dvorak (33 %), Jiri Libich, Stanislav Zvanovec. Combined Measured Characteristics of Microwave Radiometer and Free-Space Optical Link, IEEE AP-S/URSI Conference - Paper #2121. 26-30 Mar 2012.

Publikace ostatní:

Petr Dvorak (50 %), Stanislav Zvanovec. On the Sensitivity of Fire Detection by a Microwave Radiometer, IEEE International Geoscience and Remote Sensing Symposium, Melbourne, Australia,. Vol. 3, pp.402-405.4, 21-26. July 2013.

Jiri Libich, Martin Mudroch, Petr Dvorak (25 %), Stanislav Zvanovec, „Performance Analysis of Hybrid FSO/RF Link" EuCAP 2012: the 6th Conference on Antennas and Propagation, Prague, 2012.

Petr Dvorak (25 %), Federico Alimenti, Paolo Mezannotte, Luca Roselli. 31.4GHz BEOL Embedded BiCMOS MEMS Switch, Barcelona, Spain /7th MC Meeting and Workshop of COST IC0803, September 19, 2011.

Petr Dvorak (100 %), Radiometer Based Subsystem for On-line Atmosphere Monitoring 5th Management Committee/Working Group Meeting and Workshop - November 8-9, 2010, Ecole Polytechnique Fédérale de Lausanne, CH-105 Lausanne, Switzerland

Publikace ostatní

Publikace v impaktovaných časopisech:

Jiri Libich, Petr Dvorak (25 %), Petr Piksa, Stanislav ZVANOVEC, „Correction of Thermal Deviations in Fabry-Perot Resonator Based Measurements of Specific Gases in Millimeter Wave Bands", Radioengineering, submitted 17th November 2011 and accepted.

Publikace v recenzovaných časopisech

Patenty

Publikace excerpované WOS

Publikace ostatní

Procentuální podíl všech spoluautorů u uvedených publikací je rovnoměrný.

Summary

In this thesis new methodologies of remote sensing from the radiometric point of view will be described. The main thesis focus consists of two parts, the first part deals with the new methodology of atmosphere dynamic effects (rain, clouds) sensing. The methodology is based on evaluation of brightness temperature variance. Next, methodology of fire remote detection and it's properties from the microwave point of view is proposed. Fire emissivity, other properties and environmental parameters are examined and described.

Keywords: radiometry, atmosphere sensing, rain prediction, fire sensing.

Resumé

V teto dizertační tezi jsou popsány nové metodiky dálkového průzkumu z pohledu radiometrie. Hlavní práce je složena ze dvou částí. První část popisuje novou metodiku měření atmosférických dynamických jevů (deště, oblačnost). Metodika je založena na vyhodnocení rozptylu měřené jasové teploty. V druhé části je navržena nová metodika dálkové detekce ohně na základě mikrovlnných vlastností prostředí a samotného ohně. Všechny tyto parametry a vlastnosti jsou prozkoumány a popsány.

Keywords: radiometrie, průzkum atmosféry, předpověd deště, detekce ohně.